

Increased Activity of the Vacuolar Monosaccharide Transporter TMT1 Alters Cellular Sugar Partitioning, Sugar Signaling, and Seed Yield in Arabidopsis^{1[OA]}

Karina Wingenter, Alexander Schulz, Alexandra Wormit, Stefan Wic, Oliver Trentmann, Imke I. Hoermiller, Arnd G. Heyer, Irene Marten, Rainer Hedrich, and H. Ekkehard Neuhaus*

Pflanzenphysiologie, Technische Universität Kaiserslautern, D-67653 Kaiserslautern, Germany (K.W., A.W., S.W., O.T., H.E.N.); Botanik, Molekulare Pflanzenphysiologie und Biophysik, Julius-von-Sachs-Institut, Julius-Maximilians-Universität Würzburg, D-97082 Würzburg, Germany (A.S., I.M., R.H.); and Botanik, Institut für Biologie, Universität Stuttgart, D-70569 Stuttgart, Germany (I.I.H., A.G.H.)

The extent to which vacuolar sugar transport activity affects molecular, cellular, and developmental processes in Arabidopsis (*Arabidopsis thaliana*) is unknown. Electrophysiological analysis revealed that overexpression of the tonoplast monosaccharide transporter TMT1 in a *tmt1-2::tDNA* mutant led to increased proton-coupled monosaccharide import into isolated mesophyll vacuoles in comparison with wild-type vacuoles. *TMT1* overexpressor mutants grew faster than wild-type plants on soil and in high-glucose (Glc)-containing liquid medium. These effects were correlated with increased vacuolar monosaccharide compartmentation, as revealed by nonaqueous fractionation and by *chlorophyll_{ab}-binding protein1* and *nitrate reductase1* gene expression studies. Soil-grown *TMT1* overexpressor plants respired less Glc than wild-type plants and only about half the amount of Glc respired by *tmt1-2::tDNA* mutants. In sum, these data show that TMT activity in wild-type plants limits vacuolar monosaccharide loading. Remarkably, *TMT1* overexpressor mutants produced larger seeds and greater total seed yield, which was associated with increased lipid and protein content. These changes in seed properties were correlated with slightly decreased nocturnal CO₂ release and increased sugar export rates from detached source leaves. The *SUC2* gene, which codes for a sucrose transporter that may be critical for phloem loading in leaves, has been identified as Glc repressed. Thus, the observation that *SUC2* mRNA increased slightly in *TMT1* overexpressor leaves, characterized by lowered cytosolic Glc levels than wild-type leaves, provided further evidence of a stimulated source capacity. In summary, increased TMT activity in Arabidopsis induced modified subcellular sugar compartmentation, altered cellular sugar sensing, affected assimilate allocation, increased the biomass of Arabidopsis seeds, and accelerated early plant development.

Sugars fulfill an extraordinarily wide range of functions in plants as well as in other organisms. They serve as valuable energy resources that are easy to store and remobilize. Sugars are required for the synthesis of cell walls and carbohydrate polymers. They are also necessary for starch accumulation and serve as precursors for a range of primary and secondary plant intermediates. From a chemical point of view, sugars represent a large class of metabolites. Among the prominent members in higher plants are the monosaccharides Glc and Fru and the disaccharide Suc (ap Rees, 1994).

In contrast to heterotrophic organisms, plants are able to synthesize sugars *de novo* and to degrade them via oxidative or fermentative metabolism (Heldt, 2005). Net sugar accumulation in plants takes place during the day, whereas net degradation of stored carbohydrate reserves takes place the following night. In higher plants, autotrophic and heterotrophic organs appear to be interconnected by phloem for long-distance transport of sugars (Ruiz-Medrano et al., 2001). Accordingly, sugars must be transported within cells, between cells, and between plant organs. Given these factors, along with the outstanding importance of sugars, it is not surprising that plants sense intracellular sugar availability and use this information to coordinate the expression of many genes (Koch, 1996; Moore et al., 2003).

In Arabidopsis (*Arabidopsis thaliana*), about 60 genes code for putative monosaccharide transport proteins and about 10 genes encode predicted disaccharide carriers (Lalonde et al., 2004). Transport of neutral sugars has been monitored across the plasma membrane, the chloroplast envelope, and the vacuolar membrane (Weber et al., 2000; Niitylä et al., 2004; Martinoia et al., 2007). So far, all sugar carriers residing in the plant plasma membrane have been character-

¹ This work was supported by the Deutsche Forschungsgemeinschaft (Forschergruppe grant no. 1061 to H.E.N. and R.H.) and by the Landesstiftung Baden Württemberg (grant no. 33-729.64-3/28 A6 to A.G.H.).

* Corresponding author; e-mail neuhaus@rhrk.uni-kl.de.

The author responsible for distribution of materials integral to the findings presented in this article in accordance with the policy described in the Instructions for Authors (www.plantphysiol.org) is: H. Ekkehard Neuhaus (neuhaus@rhrk.uni-kl.de).

[^{OA}] Open Access articles can be viewed online without a subscription.

www.plantphysiol.org/cgi/doi/10.1104/pp.110.162040

ized to catalyze proton-coupled sugar movement (Sauer, 1992; Büttner and Sauer, 2000; Carpaneto et al., 2005). In contrast, both facilitated diffusion and proton-driven antiport mechanisms have been described for monosaccharide and Suc transport across the vacuolar membrane (Thom and Komor, 1984; Daie and Wilusz, 1987; Martinoia et al., 1987; Shiratake et al., 1997; Neuhaus, 2007).

In plants, vacuoles fulfill critical functions in the long-term and temporary storage of sugars, sugar alcohols, and other primary metabolites such as carboxylates and amino acids (Dietz et al., 1990; Rentsch and Martinoia, 1991; Martinoia and Rentsch, 1992; Emmerlich et al., 2003). Recently, the first solute carriers responsible for vacuolar Suc and inositol transport have been identified (Endler et al., 2006; Schneider et al., 2008). In addition, TMT (for tonoplast monosaccharide transporter) and VGT (for vacuolar Glc transporter) were the first vacuolar carrier proteins proven to have transport capacity for both Glc and Fru (Wormit et al., 2006; Aluri and Büttner, 2007).

TMT exists in three isoforms in Arabidopsis (TMT1–TMT3), and orthologs have been found in other plant species like grapevine (*Vitis vinifera*), barley (*Hordeum vulgare*), and rice (*Oryza sativa*; Wormit et al., 2006). In Arabidopsis, the genes *TMT1* and *TMT2* are expressed in various tissues, whereas *TMT3* is hardly expressed throughout the entire plant life cycle (Wormit et al., 2006). Interestingly, *TMT1* and *TMT2* are induced by Glc, salt, drought, and cold stress (Wormit et al., 2006), and vacuoles isolated from a *TMT1* loss-of-function (*T-DNA*) Arabidopsis mutant showed reduced Glc import capacity in comparison with corresponding wild-type organelles (Wormit et al., 2006). Moreover, after transfer into the cold, these mutant leaves showed impaired ability to accumulate Glc and Fru, underscoring the *in vivo* function of TMT under selected conditions (Wormit et al., 2006).

However, it is unknown to what extent overexpression of a vacuolar sugar carrier affects subcellular sugar allocation in Arabidopsis. In addition, whether increased vacuolar sugar transport influences sugar signaling, plant development, or organ properties has not been determined. Thus, it is unknown how important controlled activity of vacuolar monosaccharide transport is to plant development or physiological properties. To reveal whether TMT activity affects these processes, we created *TMT1*-overexpressing Arabidopsis lines and analyzed their physiological and molecular feedbacks.

RESULTS

Generation of *TMT1* Overexpressor Lines

To gain increased monosaccharide import into Arabidopsis vacuoles, the *TMT1* gene was expressed under the control of a constitutive cauliflower mosaic

virus 35S promoter. To prevent possible cosuppression, we transformed the homozygous Arabidopsis mutant *tmt1-2::tDNA* lacking isoforms TMT1 and TMT2. Sugar levels and physiological properties of this double mutant are nearly identical to the triple mutant *tmt1-2-3::tDNA* lacking all TMT isoforms (Wormit et al., 2006). The *TMT1*-overexpressing lines 1, 4, and 10 were selected from 25 independent 35S:*tmt1*;1-2 mutants on the basis of high *TMT1* mRNA levels (Fig. 1A).

When grown at standard temperature (21°C), *TMT1* mRNA was not detectable in the *tmt1-2::tDNA* mutant or in wild-type plants (Fig. 1A). The absence of detectable *TMT1* mRNA in wild-type plants and the *tmt1-2::tDNA* line is consistent with both the homozygous situation in the knockout mutant and the low *TMT1* expression level in leaves of Arabidopsis plants grown at standard temperature (Wormit et al., 2006). However, the *TMT1* gene is cold induced (Wormit et al., 2006), and upon transfer of the plants into the cold (4°C), we were able to detect *TMT1* mRNA in wild-type leaves but not in the *tmt1-2::tDNA* mutant (Fig. 1B). In comparison with wild-type plants, it was evident that even under cold conditions the 35S:*tmt1*;1-2 mutant lines 1, 4, and 10 exhibited severalfold increases in *TMT1* mRNA (Fig. 1B).

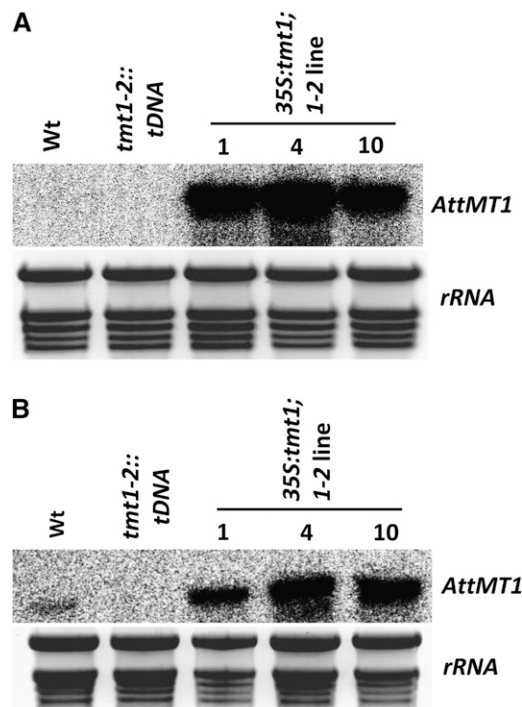


Figure 1. Quantification of mRNA coding for TMT1 in Arabidopsis leaf samples from wild-type (Wt), *tmt1-2::tDNA*, and 35S:*tmt1*;1-2 plants. A, Plants were grown for 6 weeks. B, Plants were grown for 6 weeks and subsequently incubated for 2 d at 4°C before RNA isolation. rRNA is displayed as loading control.

Patch-Clamp Analysis of Isolated Vacuoles from Arabidopsis Plants

Previously, we showed that all TMT proteins reside in the vacuolar membrane and that they are very likely involved in Glc accumulation in vacuoles (Wormit et al., 2006). Accordingly, one would expect that this TMT-mediated importing of Glc into vacuoles is energized by the pH gradient across the vacuolar membrane. Electrogenic-type sugar transport across the membrane of Arabidopsis mesophyll vacuoles has recently been identified and characterized with the patch-clamp technique (Schneider et al., 2008). Therefore, to provide evidence for the function of TMT proteins as vacuolar Glc-uptake carrier systems, whole-vacuole patch-clamp measurements were conducted to resolve small current amplitudes expected for transporters with low transport capacity.

Since the transport capacity of H⁺-dependent carrier systems is likely to depend on both the substrate and the H⁺ gradient across the membrane, the first set of experiments was performed in the presence of a physiological pH gradient from pH 5.5 in the vacuolar lumen to pH 7.5 in the cytosol (Fig. 2A, top panel). When the Glc gradient was raised 50-fold upon increasing the Glc concentration in the cytosolic medium from 0 to 50 mM (Fig. 2A, top panel), there was a simultaneous rise in negative current (Fig. 2, A, bottom panel, and B). This points to Glc/substrate-driven H⁺ currents directed from the vacuole into the cytosol. Under identical experimental conditions, *TMT1*-overexpressing vacuoles from 35S:*tmt1;1-2* mutant line 4 exhibiting the highest corresponding mRNA accumulation showed a 2-fold higher response to Glc application than wild-type vacuoles (Fig. 2, A, bottom panel, and B). In contrast, only minor Glc-induced currents were recorded from vacuoles of the double mutant *tmt1-2::tDNA* (Fig. 2, A, bottom panel, and B).

These results suggest that TMT1 functions as an electrogenic transporter that mediates Glc import into the vacuole and H⁺ export out of the vacuole. To further explore the pH dependence of this transport system, additional experiments with TMT1-overexpressing vacuoles were performed under symmetrical pH conditions. With a pH of 7.5 on both sides of the membrane, Glc-induced H⁺ currents were about 50% lower in comparison with the pH gradient (Fig. 2C). These observations indicate that (1) TMT1-mediated Glc uptake into the vacuole is strongly promoted by a pH gradient in the opposite direction to the Glc gradient, and (2) a sole Glc gradient can drive TMT1-mediated H⁺ flux from the vacuole into the cytosol.

Growth of *TMT1* Overexpressors in Liquid Culture

The electrophysiological analysis demonstrated that overexpression of the *TMT1* gene induces an increase in Glc transport capacity in isolated mutant vacuoles (Fig. 2, A and B). To determine whether increased vacuolar Glc import activity affects plant performance,

we incubated wild-type plants, *tmt1-2::tDNA* mutants, and all three 35S:*tmt1;1-2* overexpressor lines (Fig. 1) in liquid culture medium with and without Glc supplement.

Under standard conditions, all plant lines developed rapidly within 12 d, and the biomass of each genotype approached 185 mg (Fig. 3A). However, the presence of 5% Glc inhibited plant development, leading to less than 25 mg fresh weight of wild-type plants (Fig. 3B). The double knockout mutant *tmt1-2::tDNA* developed only slightly in the presence of Glc, attaining no more than 9 mg fresh weight within 12 d (Fig. 3B). In marked contrast, all three 35S:*tmt1;1-2* lines grew even better than the corresponding wild-type plants. Fresh weights from overexpressor mutants ranged from 49 mg (line 1) to 57 mg (line 10) to 78 mg (line 4; Fig. 3B). It should be noted that the strongest effect observed in *TMT1* overexpressor line 4 (Fig. 3B) coincided with the highest corresponding mRNA accumulation (Fig. 1).

Sugar Metabolism in Arabidopsis Plants Grown in Liquid Culture

It is well known that cell internal sugar levels govern the development of plants (Rolland et al., 2002). In contrast to control conditions, in which all plant genotypes exhibited similar development (Fig. 3A), the presence of 5% Glc in the liquid culture medium led to strongly individual responses in wild-type plants, in *tmt1-2::tDNA* plants, and in the three 35S:*tmt1;1-2* overexpressor lines tested (Fig. 3B). Thus, it was of interest to analyze sugar metabolism in these genotypes in more detail.

In the first set of analyses, we quantified total sugar levels in the wild type and in *TMT1* overexpressor lines 1, 4, and 10 (note that sugar quantification in the *tmt1-2::tDNA* mutant was impossible due to the nearly complete inhibition of growth in these plants under high-Glc conditions; Fig. 3B). Interestingly, although all *TMT1* overexpressor lines grew much better than the wild-type plants under conditions of high Glc (Fig. 3B), the fresh weight levels of Glc, Fru, and Suc in all four plant genotypes were almost equal (Fig. 4A). Glc levels were between 21 and 23 $\mu\text{mol g}^{-1}$ fresh weight, Fru levels were much lower, approaching between 2 and 3 $\mu\text{mol g}^{-1}$ fresh weight, and Suc had the highest concentrations, ranging between 27 and 31 $\mu\text{mol g}^{-1}$ fresh weight (Fig. 4A). Thus, on the basis of total sugar levels, we cannot explain why all 35S:*tmt1;1-2* mutant lines grew better than wild-type plants at high Glc concentrations.

It was necessary to analyze subcellular sugar partitioning with "nonaqueous fractionation." This method allows the determination of subcellular partitioning of metabolites in leaves of Arabidopsis and other plant species (Gerhardt and Heldt, 1984; Dancer et al., 1990; Farre et al., 2000; Fettke et al., 2005). Wild-type Arabidopsis plants grown in high-Glc liquid culture medium and exhibiting reduced biomass relative to

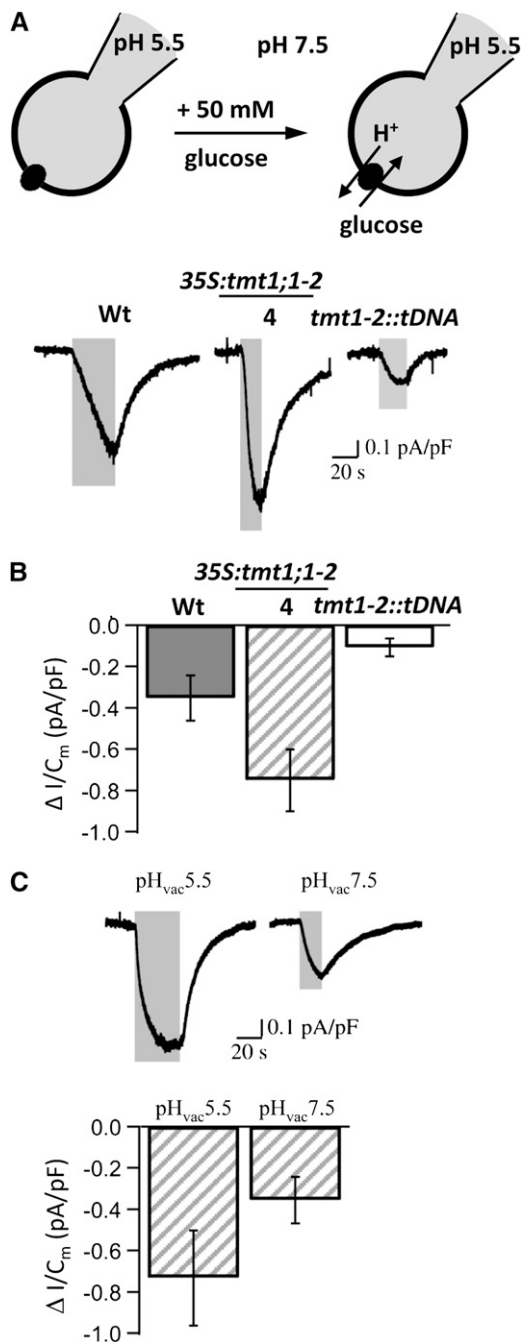


Figure 2. Whole-vacuole recordings of Glc-triggered proton currents in mesophyll vacuoles of wild-type (Wt) and *TMT* mutant plants. **A**, The cartoon shows the experimental conditions at pH 5.5 in the vacuolar lumen (pipette) and pH 7.5 in the cytosol (bath) in the absence (left) and presence (right) of 50 mM Glc. Representative current traces recorded from vacuoles of wild-type, *TMT1*-overexpressing line 4 (*35S:tmt1;1-2*), and *tmt1-2::tDNA* plants are given below the cartoon. Cytosolic Glc treatment indicated by the superimposed gray bars resulted in downward deflection of the current trace. **B**, Sugar-induced changes in current density determined from individual vacuoles under conditions identical to those in **A** are given as means \pm SE. Number of experiments was $n = 14$ for wild-type (gray bar), $n = 12$ for the *TMT1*-overexpressing line 4 (striped bar), and $n = 9$ for *tmt1-2::tDNA* (white bar) vacuoles. Data comprise Glc-induced current responses from vacuoles isolated

control plants (Fig. 3B) stored about 40% of the Glc in the vacuole, 43% in the plastid, and 17% in the cytosol (Fig. 4B). In contrast, *35S:tmt1;1-2* line 1 accumulated more than 80% of the Glc in the vacuole, 20% in the plastids, and less than 1% (lower detection limit) in the cytosol. Similarly, *35S:tmt1;1-2* line 4 accumulated 65% of the Glc in the vacuole, 35% in the plastids, and no detectable amount in the cytosol (Fig. 4B). A similarly altered sugar accumulation pattern was evident for Fru. Wild-type plants contained about 45% of the Fru in the vacuole, 31% in the plastids, and 24% in the cytosol. *TMT1* overexpressor lines 1 and 4 accumulated Fru nearly exclusively in the vacuole, which held up to 90% (line 1), whereas less than 10% occurred in plastids (Fig. 4B). These lines did not accumulate Fru in the cytosol (Fig. 4B).

Altered Gene Expression in *TMT1* Overexpressor Plants Grown in Liquid Culture

Cellular sugars are known effectors of plant gene expression (Rolland et al., 2002). The gene coding for *chlorophyll_{ab}-binding protein1* (*CAB1*) is repressed by Glc, whereas the *nitrate reductase1* gene (*NR1*) is Glc induced (Koch, 1996). To verify whether the observed altered sugar partitioning in *TMT1* overexpressor lines (Fig. 4B) affects the expression of these genes, we used northern-blot analysis to compare *CAB1* and *NR1* mRNA accumulation in plants grown under either standard liquid-culture conditions or conditions of high Glc (Fig. 5).

When grown in liquid culture medium lacking additional Glc, wild-type plants and all three *35S:tmt1;1-2* lines had similar levels of *CAB1* and *NR1* mRNAs (Fig. 5, top panel). However, the presence of Glc during growth in liquid culture reduced *CAB1* mRNA in wild-type plants much more than in *TMT1* overexpressor mutants, leading to higher *CAB1* mRNA in *35S:tmt1;1-2* lines 1, 4, and 10 (Fig. 5, bottom panel). In contrast, the presence of Glc in the liquid culture medium activated *NR1* gene expression in wild-type plants more than in *TMT1* overexpressor lines, leading to less *NR1* mRNA in *35S:tmt1;1-2* lines 1, 4, and 10 in comparison with corresponding wild-type plants (Fig. 5, bottom panel).

from leaves without and with preincubation in 100 mM Glc. Note that similar Glc-induced current densities were recorded under different Glc preconditions (data not shown). **C**, pH dependence of Glc-triggered proton currents in mesophyll vacuoles of *TMT1*-overexpressing line 4. Representative current traces recorded at pH 7.5 in the cytosol and either pH 7.5 or 5.5 in the lumen are shown. Cytosolic Glc treatment (50 mM) is indicated by the superimposed gray bars. Current responses were obtained from vacuoles isolated from leaves without Glc preincubation. Average Glc-induced current densities \pm SE determined under symmetrical and asymmetrical pH conditions are given below the individual current recordings. Number of experiments was $n = 6$ for pH 5.5 and $n = 8$ for pH 7.5 in the vacuolar lumen.

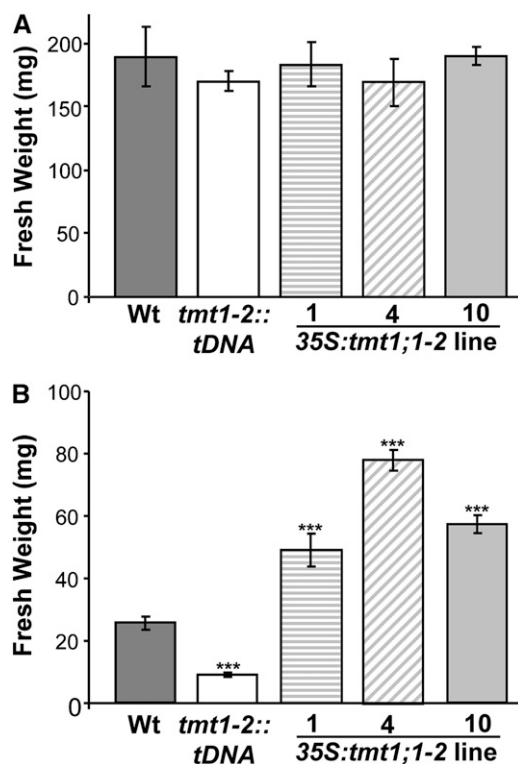


Figure 3. Fresh weight of wild-type (Wt) and *TMT1* mutant Arabidopsis plants grown in liquid culture. A, Plants were grown for 7 d in liquid culture medium. B, Plants were grown for 7 d in liquid culture medium plus 5% Glc. Dark gray bars represent wild-type samples, white bars represent *tmt1-2::tDNA*, striped bars represent *35S:tmt1;1-2* line 1, diagonal striped bars represent line 4, and light gray bars represent line 10. Asterisks above the bars report the results of a significance test (Student's *t* test) for differences between the *TMT* mutants and the wild type: *** $P < 0.005$. Each data point represents the mean of three independent biological experiments \pm SE.

Respiration of Newly Imported Glc, and Expression of *CAB1* and *NR1* in Soil-Grown Arabidopsis

In Figure 4B, we reported altered subcellular sugar compartmentation in *TMT1* overexpressor plants. To reveal whether these alterations were correlated with changing respiratory properties, we prepared soil-grown seedlings 9 d after germination and incubated these plants in $100 \mu\text{M}$ ^{14}C -labeled Glc (Fig. 6A).

Wild-type plants respired 18% of newly imported Glc within 6 h of incubation, whereas *tmt1-2::tDNA* mutants showed a significant increase in respiratory consumption, approaching 26% (Fig. 6A). In contrast, all *35S:tmt1;1-2* lines exhibited less $^{14}\text{CO}_2$ release from newly imported radioactively labeled Glc, ranging from 13% in mutant line 1 to 14% in mutant line 4 (Fig. 6A).

To determine the expression of sugar-affected genes in soil-grown Arabidopsis *TMT* mutants, we quantified *CAB1* and *NR1* mRNA accumulation by quantitative reverse transcription (qRT)-PCR (Fig. 6B). For this analysis, leaf samples were prepared and total

mRNA was isolated and transcribed to cDNA prior to qPCR. Leaves from *tmt1-2::tDNA* plants accumulated about 68% of the *CAB1* mRNA present in wild-type tissues, whereas all three independent *35S:tmt1;1-2* lines exhibited increased *CAB1* mRNA concentrations (Fig. 6B). In contrast, *NR1* mRNA in *tmt1-2::tDNA* plants increased by about 50% in comparison with the content in wild-type plants, whereas all three *tmt1-*

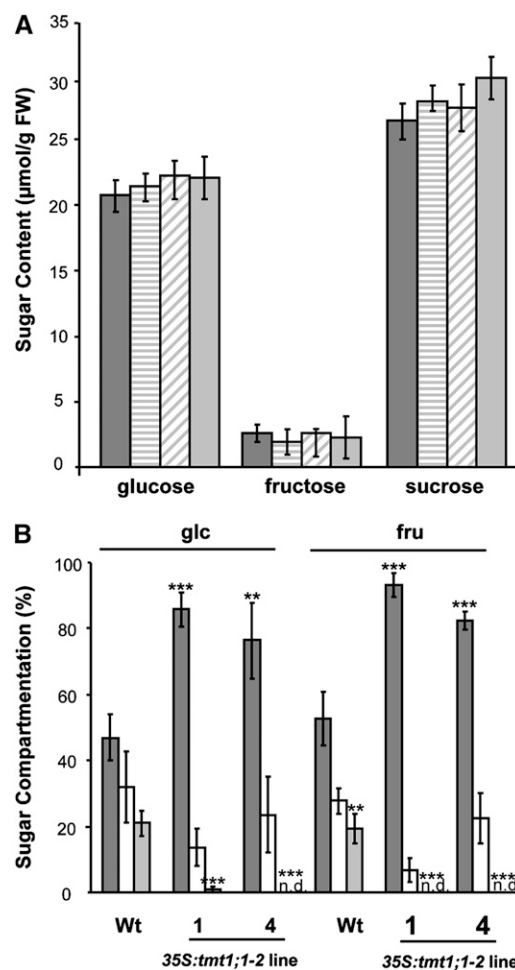


Figure 4. Sugar levels and sugar compartmentation in Arabidopsis seedlings grown in liquid culture. A, Sugar content in seedlings from 7-d-old wild-type (Wt) and *35S:tmt1;1-2* plants grown in liquid medium supplemented with 5% Glc. Dark gray bars represent wild-type samples, white bars represent *tmt1-2::tDNA*, striped bars represent *35S:tmt1;1-2* line 1, diagonal striped bars represent line 4, and light gray bars represent line 10. Data represent means of three independent experiments \pm SE. FW, Fresh weight. B, Seedlings were grown in liquid medium supplemented with 5% Glc. Sugar compartmentation was analyzed via nonaqueous fractionation. Dark gray bars represent the vacuole, white bars represent the plastid, and light gray bars represent the cytosol. Data represent means of two independent experiments \pm SE, each consisting of three individual plants. Note that in some samples, we calculated more than 100% of total sugar due to SE. Asterisks above the bars report the results of a significance test (Student's *t* test) for differences between the *TMT* mutants and the wild type: *** $P < 0.005$, ** $P < 0.01$.

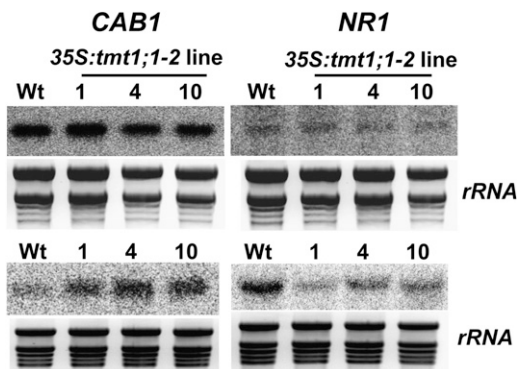


Figure 5. Quantification of mRNA coding for *CAB1* or *NR1* in seedling samples from wild-type (Wt) plants and *35S:tmt1;1-2* lines 1, 4, and 10. Seedlings were grown in liquid culture for 7 d, and total RNA was isolated and probed for the relative abundance of mRNA coding for *CAB1* or *NR1*. rRNA represents the loading control. The top panel shows levels of *CAB1* and *NR1* mRNA in seedlings grown in standard medium. The bottom panel shows levels of *CAB1* and *NR1* mRNA in seedlings grown in medium where 5% Glc was added.

2::*tDNA* plants had substantially reduced *NR1* mRNA levels (Fig. 6B). Although the observed changes in *CAB1* and *NR1* expression were quite small, they were statistically significant (Fig. 6B) and they fully confirmed the corresponding expression changes observed in plant lines grown in Glc-supplemented liquid culture medium (Fig. 5).

Growth Pattern of Arabidopsis *TMT* Mutants under Standard Conditions

To determine whether altered *TMT1* activity influences the development of Arabidopsis, we grew wild-type and *TMT* mutant plants for 15 or 34 d on soil and monitored the resulting plant phenotypes. *tmt1-2::tDNA* plants developed slower than wild-type plants within the first 15 d, whereas all three *TMT1* over-expressor lines grew faster than wild-type plants (Fig. 7A). These phenotypic differences among the five plant lines were still evident, but less pronounced, in plants grown for 34 d (Fig. 7B).

Seed Properties and Composition of Arabidopsis Plants with Altered *TMT1* Activity

To reveal whether different seed properties of *TMT1* mutants contributed to the developmental changes observed during the early phase of growth (Fig. 7), we analyzed corresponding seeds in detail. A rapid measure of general seed properties is the analysis of the "1,000 seed weight." Seeds collected from *tmt1-2::tDNA* plants exhibited a small reduction in 1,000 seed weight, approaching 90% of the weight observed in wild-type seeds (Fig. 8A). In marked contrast, all three *35S:tmt1;1-2* lines produced seeds exhibiting significantly higher weight. *35S:tmt1;1-2* line 1 plants produced seeds that were 13% heavier than wild-type

seeds, line 4 exhibited seeds that were 28% heavier than wild-type seeds, and line 10 plants produced seeds that were 25% heavier than wild-type seeds (Fig. 8A).

Arabidopsis seeds consist mainly of lipids and proteins (Li et al., 2006). For this reason, it was of interest to determine whether the changes in 1,000 seed weight were caused by changes in a specific storage component or by alterations in both major storage compounds. Seeds from *tmt1-2::tDNA* plants contained about 10% less lipids and proteins than wild-type seeds (Fig. 8, B and C), whereas the three *35S:tmt1;1-2* lines contained significantly higher lipid and protein levels (Fig. 8, B and C), whereas the three *35S:tmt1;1-2* line 1 seeds contained slightly more lipids (+5% compared with wild-type seeds) and about 11% more storage

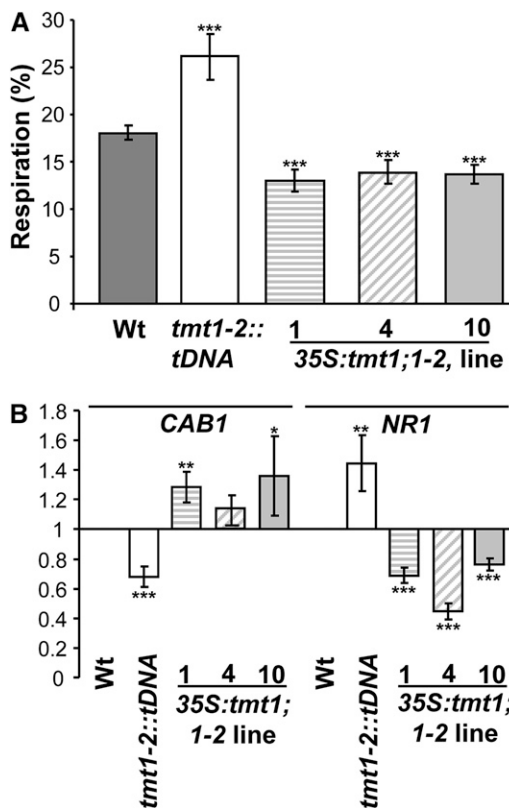


Figure 6. Respiratory activity, intracellular sugar compartmentation, and gene expression in Arabidopsis wild-type (Wt) and *TMT* mutant plants. A, Respiration of [¹⁴C]Glc in 3-week-old Arabidopsis seedlings. Plants were grown on soil under standard conditions. Dark gray bars represent wild-type samples, white bars represent *tmt1-2::tDNA*, striped bars represent *35S:tmt1;1-2* line 1, diagonal striped bars represent line 4, and light gray bars represent line 10. Data given represent means of four individual experiments, each with five replicate samples \pm SE. B, qRT-PCR was used to validate the expression level of *CAB1* and *NR1* in soil-grown Arabidopsis leaves. Data represent means of three independent experiments \pm SE. Asterisks above and below the bars report the results of a significance test (Student's *t* test) for differences between the *TMT* mutants and the wild type: *** $P < 0.005$, ** $P < 0.01$, * $P < 0.5$.



Figure 7. Growth of Arabidopsis wild-type (Wt) and *TMT* mutant plants on soil. Arabidopsis plants were grown under standard conditions (21°C) on soil. Results are shown at 15 d after germination (A) and 34 d after germination (B).

protein. *35S:tmt1;1-2* line 4 contained about 4.9 μg of lipid per seed, representing an increase of nearly 12%, and 14% more storage protein. Seeds collected from *35S:tmt1;1-2* line 10 had about 12% more lipids and 10% more storage protein than wild-type seeds (Fig. 8, B and C). These data illustrate that the increased 1,000 seed weight in *TMT1* overexpressor plants (Fig. 8A) resulted from increases in both lipids and proteins.

To explore whether the altered 1,000 seed weight in *TMT1* mutants was correlated with altered total seed yield, we conducted two types of analysis. First, we counted the developing seeds per single silique. Second, we weighted whole seeds collected from single *TMT1* mutants. As shown in Figure 8D, wild-type plants and all *TMT* mutants (double mutants and the three *TMT1* overexpressor lines tested) produced highly similar numbers of seeds, approximately 42 seeds per silique, without significant differences (Fig. 8D). The entire number of siliques per plant was not altered (data not shown). However, the total seed harvest per plant was altered in both the *tmt1-2::tDNA* plants and the three *35S:tmt1;1-2* mutants in comparison with wild-type plants. The latter produced an average of 125 mg of seeds per plant, whereas *tmt1-2::tDNA* mutants produced an average of 101 mg of seeds per plant (Fig. 8E). In marked contrast, all three *35S:tmt1;1-2* mutants produced a higher seed mass than wild-type plants. *35S:tmt1;1-2* line 1 produced 218 mg of seeds per plant, *35S:tmt1;1-2* line 4 produced 178 mg of seeds per plant, and *35S:tmt1;1-2* line 10 produced 157 mg of seeds per plant (Fig. 8E).

Rates of Photosynthesis and Nocturnal Respiration in Arabidopsis Wild-Type Plants and *TMT* Mutant Lines

To reveal whether altered gene expression (Fig. 6C) and increased total seed biomass in *TMT1* overexpressor plants (Fig. 8, A and E) were correlated with altered carbon exchange rates in leaves, we quantified daily rates of net photosynthesis and nocturnal CO_2 release in aerial plant organs (Fig. 9). During the light

phase, wild-type plants, *tmt1-2::tDNA*, and *35S:tmt1;1-2* line 1 did not show a difference in average CO_2 fixation (Fig. 9A), while *35S:tmt1;1-2* lines 4 and 10 (exhibiting the highest seed yield gains in comparison with wild-type plants; Fig. 8, A and E) showed slightly higher rates of CO_2 fixation (Fig. 9A). However, nocturnal CO_2 release of aerial organs in *35S:tmt1;1-2* lines 4 and 10 was significantly lower than in the wild type and the *tmt1-2::tDNA* double knockout line (Fig. 9B). When compared with wild-type plants, *TMT1* overexpressor line 1 exhibited a slight, but statistically nonsignificant, reduction in average CO_2 release during the night phase (Fig. 9B).

Sugar Export by Wild-Type and *TMT* Mutant Leaves, and *SUC2* Expression Analysis

Enhanced seed biomass might result from increased transfer of carbohydrates from source leaves to sink structures. It has been suggested that the Arabidopsis Suc transporter *SUC2* is critical for phloem loading (Truernit and Sauer, 1995). Assuming that *SUC2* is involved in increased sugar loading into phloem cells from source leaves, we first analyzed how sugars affect *SUC2* expression.

To accomplish this, we incubated leaf discs from wild-type plants for 4 or 16 h in Glc-containing water and monitored *SUC2* mRNA accumulation via qRT-PCR (Fig. 10A). The application of Glc led to a decrease in *SUC2* transcript of about 50% within 4 h; after 16 h of Glc application, the *SUC2* transcript approached 10% of the value at the beginning of the experiment (Fig. 10A). Controls with pure water did not lead to altered *SUC2* mRNA accumulation of this sort (data not shown).

To analyze whether *SUC2* mRNA in *TMT* mutant leaves differed from corresponding wild-type tissues, we isolated total mRNA from 6-week-old plants and conducted qRT-PCR analysis. Leaves from *tmt1-2::tDNA* plants accumulated about 75% of *SUC2* mRNA levels in wild-type tissues, whereas all three independent *35S:tmt1;1-2* lines exhibited increased *SUC2* mRNA, approaching about 150% of levels in wild-type leaf tissue in line 4 (Fig. 10B).

Phloem export capacity of detached source leaves was quantified to gain information on putatively altered sugar export properties in *TMT* mutant lines. In this analysis, we cut leaves from corresponding plants at the end of the light phase, recut petiole ends under water, transferred petioles directly into reaction tubes filled with 200 μL of 15 mM EDTA (pH 7.5; Tedone et al., 2004), and determined the amount of sugar (sum of Suc, Glc, and Fru) released within 16 h of dark incubation (Fig. 10C). Within this dark phase, detached wild-type leaves exported about 12.5 $\mu\text{mol C}_6$ units g^{-1} fresh weight, whereas *tmt1-2::tDNA* double knockout leaves had a slight decrease in sugar export, amounting to 11.1 $\mu\text{mol C}_6$ units g^{-1} fresh weight (Fig. 10C). Interestingly, all three *TMT1* overexpressor lines exhibited significantly increased rates of sugar export,

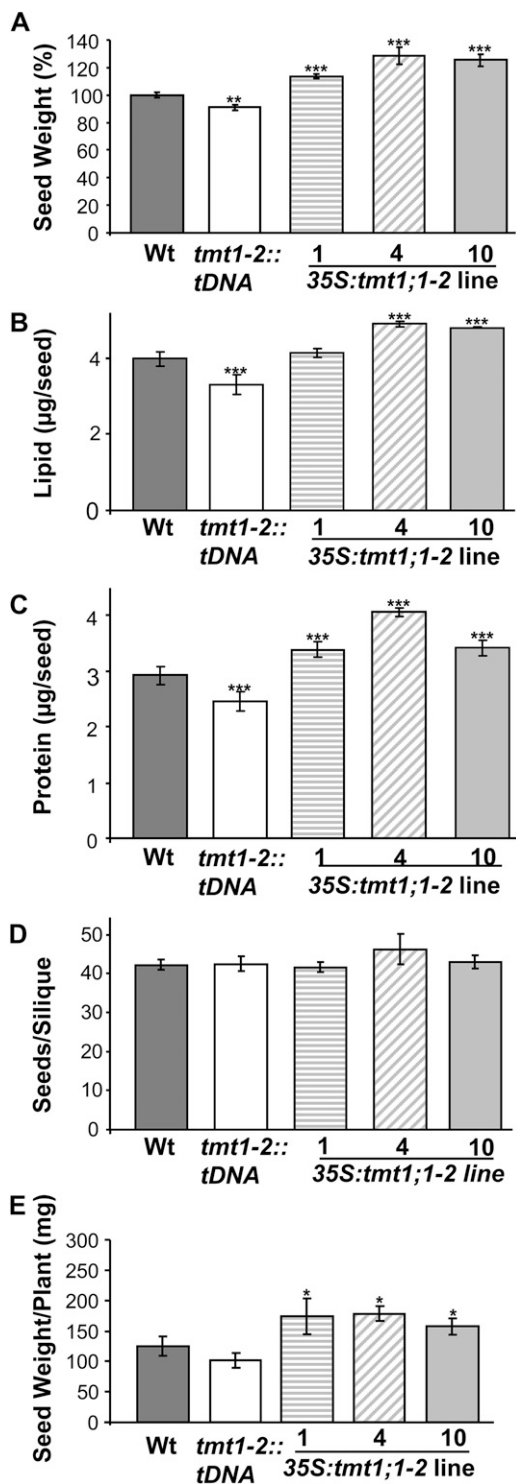


Figure 8. Seed quality analysis of wild-type (Wt) plants and *TMT* mutants. Plants were grown for 35 d on soil under short-day conditions. Subsequently, the light phase was prolonged to induce flowering (16 h of light) until the life cycle was completed. Seeds from wild-type, *tmt1-2::tDNA*, and *35S:tmt1;1-2* lines 1, 4, and 10 were collected. Data shown are for 1,000 seed weight (A), lipid content (B), protein content (C), seeds per silique (D), and entire seed weight per plant (E). Dark gray bars represent wild-type samples, white bars represent *tmt1-2::tDNA*, striped bars represent *35S:tmt1;1-2* line 1, diagonal striped bars rep-

ranging from 16.6 to 17.9 $\mu\text{mol C6 units g}^{-1}$ fresh weight (Fig. 10C).

DISCUSSION

Given the importance of sugar allocation and storage to plant metabolism, plant development, and for animal and human diets, it may be challenging to modify sugar storage capacities by molecular genetic approaches. Although it has been demonstrated that sugar deposition in vacuoles in the form of fructans greatly enhances leaf storage capacity (Pollock, 1986), the extent to which sugar transport across the vacuolar membrane limits plant performance has not been determined. To address this issue, we created *TMT1*-overexpressing Arabidopsis mutants (Fig. 1) and analyzed their properties in detail.

Overexpression of the *TMT1* gene is correlated with expected altered vacuolar monosaccharide transport activities. This conclusion is based on indirect and direct experimental evidence. First, all *TMT1* overexpressor lines exhibit decreased rates of $^{14}\text{CO}_2$ release after import of radioactively labeled Glc in comparison with wild-type plants (Fig. 6A). In contrast to the three *TMT1* overexpressor lines, the double knockout mutant *tmt1-2::tDNA* exhibits increased rates of $^{14}\text{CO}_2$ release (Fig. 6A). Second, *TMT1* overexpressor lines exhibit increased relative vacuolar monosaccharide levels in comparison with wild-type plants (Fig. 4B). In contrast, the double knockout mutant *tmt1-2::tDNA* exhibits increased cytosolic monosaccharide levels in comparison with wild-type plants (Fig. 4B). Third, patch-clamp experiments confirm stimulated Glc transport rates across the vacuolar membrane from *TMT1* overexpressor line 4 but decreased vacuolar Glc transport across vacuoles isolated from the *TMT* double mutant *tmt1-2::tDNA* (Fig. 2B).

Both the occurrence of Glc-dependent electrical currents across the membrane from patched vacuoles prepared from *TMT1*-overexpressing plants (Fig. 2B) and the strong effect of a pH gradient across the tonoplast on Glc-elicited currents (Fig. 2C) clearly indicate that *TMT1*-mediated transport is coupled to a proton antiport. Moreover, the observation that vacuoles from *tmt1-2::tDNA* mutants showed only about 20% of the current observed in wild-type vacuoles (Fig. 2B) indicates that *TMT1* and *TMT2* contribute substantially to the pH-dependent monosaccharide import observed on isolated plant vacuoles in other species (Thom and Komor, 1984; Martinoia et al., 1987). In addition, this conclusion is fully in line with the impaired ability of this double mutant to

represent line 4, and light gray bars represent line 10. Data represent means of three independent growth experiments \pm SE. Asterisks above the bars report the results of a significance test (Student's *t* test) for differences between the *TMT* mutants and the wild type: *** $P < 0.005$, ** $P < 0.01$, * $P < 0.05$.

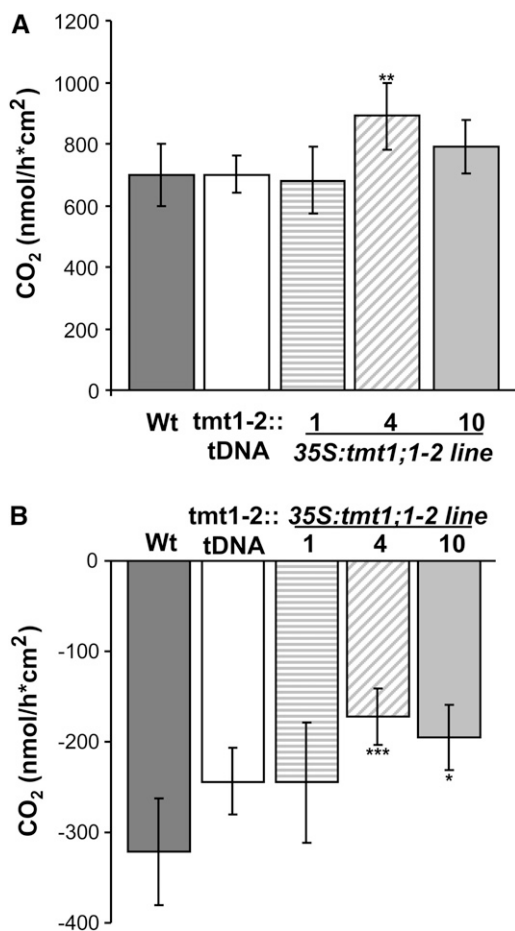


Figure 9. Quantification of photosynthesis and respiration rates. A, Photosynthetic CO₂ fixation was quantified over the entire light phase. B, Respiratory CO₂ release was quantified over the entire dark phase. Dark gray bars represent wild-type (Wt) samples, white bars represent *tmt1-2::tDNA*, striped bars represent *35S:tmt1;1-2* line 1, diagonal striped bars represent line 4, and light gray bars represent line 10. Each data point represents the mean of three individual experiments \pm SE. Asterisks above and below the bars report the results of a significance test (Student's *t* test) for differences between the *TMT* mutants and the wild type: *** $P < 0.005$, ** $P < 0.01$, * $P < 0.5$.

accumulate monosaccharides in response to cold temperature (Wormit et al., 2006). After transfer of wild-type Arabidopsis into the cold, leaf Glc and Fru levels rise about 10-fold (Wanner and Junttila, 1999; Zuther et al., 2004), whereas in the *tmt1-2::tDNA* mutant, levels of these monosaccharides increase only slightly at such temperatures (Wormit et al., 2006).

The observation that cultivation of Arabidopsis in Glc-containing liquid culture medium inhibits plant growth (Fig. 3B) exemplifies a known effect of high sugar levels on plant development (Smeekens, 1998). Since all three *35S:tmt1;1-2* mutants do not show such strong growth repression as in wild-type plants (Fig. 3B), and because the mutants contain similar total sugar levels as wild-type plants (Fig. 4A), we conclude that the absolute cellular sugar levels are of minor

importance in sugar repression of plant development. However, it is assumed that a hexokinase located in the cytosol is involved in plant sugar sensing (Xiao et al., 2000). Thus, the observation that *TMT1* over-expressor mutants, showing altered sugar signalling (Figs. 4A and 6B), do not accumulate cytosolic mono-

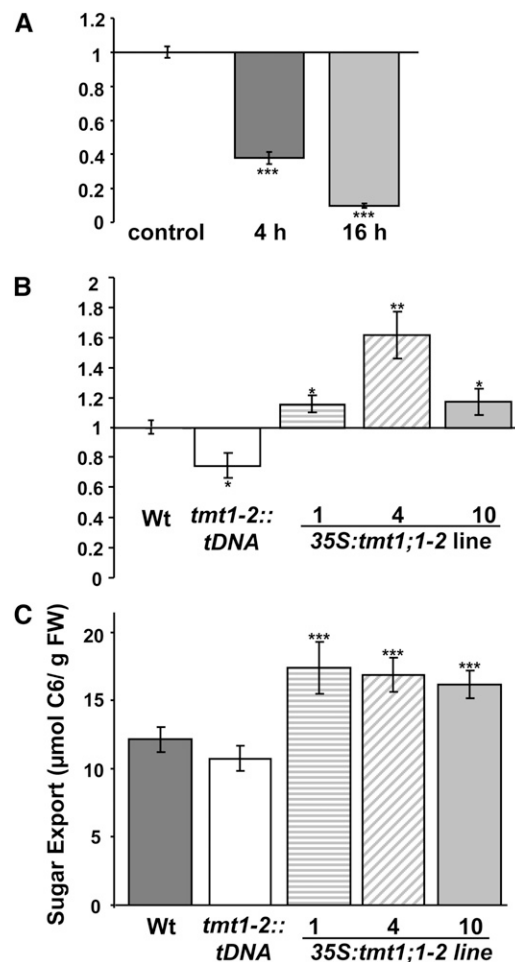


Figure 10. Expression analysis of *SUC2* and phloem exudate measurements from Arabidopsis leaves. RT-PCR was used to validate the expression profile of *SUC2*. A, Glc-induced repression of *SUC2* in wild-type (Wt) leaf discs incubated in 100 mM Glc for 4 and 16 h. Data represent means of three individual experiments \pm SE. B, Expression of *SUC2* in Arabidopsis leaves. The plants were grown 8 weeks on soil, and leaves were harvested at the end of the light phase. Data represent means of three individual experiments \pm SE. C, Sugar content of phloem exudates from detached, fully expanded Arabidopsis leaves. Arabidopsis plants were grown on soil for 8 weeks, and leaves were harvested at the end of the light phase. Exudation into 15 mM EDTA (pH 7.5) was allowed for 16 h in the dark. FW, Fresh weight. Data represent means of three independent experiments, each with six leaves. Dark gray bars represent wild-type samples, white bars represent *tmt1-2::tDNA*, striped bars represent *35S:tmt1;1-2* line 1, diagonal striped bars represent line 4, and light gray bars represent line 10. Asterisks above and below the bars report the results of a significance test (Student's *t* test) for differences between the *TMT* mutants and the wild type: *** $P < 0.005$, ** $P < 0.01$, * $P < 0.5$.

saccharides (Fig. 4B) clarifies that cytosolic Glc concentration is of superior importance in sugar regulation of gene expression. Obviously, as a consequence of the proton-energized Glc transport (Fig. 2C), *TMT1* overexpressor lines are able to build and maintain steeper monosaccharide gradients between the vacuolar lumen and the surrounding cytosol than wild-type plants (Fig. 4B).

From our data, we conclude that the activity of the tonoplast-located monosaccharide transporter TMT limits vacuolar monosaccharide accumulation in wild-type Arabidopsis plants. This conclusion appears justified for the following reasons: (1) when grown on soil, the sugar-repressed *CAB1* gene is expressed less in *tmt1-2::tDNA* plants but is expressed greater in all three *35S:tmt1;1-2* lines in comparison with wild-type plants (Fig. 6B); and (2) the sugar-induced *NR1* gene is expressed greater in *tmt1-2::tDNA* plants and expressed less in all three *35S:tmt1;1-2* lines in comparison with wild-type plants (Fig. 6B). In fact, observed changes in *CAB1* and *NR1* expression can be taken as a confirmation for altered intracellular carbohydrate partitioning, as identified by the nonaqueous fractionation of cell compartments (Fig. 4B).

Having identified Arabidopsis mutants with altered subcellular sugar partitioning and altered sensing of sugars, under both induced conditions (Figs. 4B and 5) and on soil (Fig. 6B), the challenge of analyzing the plants in greater detail remains. The decelerated development of *tmt1-2::tDNA* plants and the accelerated development of all three *35S:tmt1;1-2* lines on soil (Fig. 7) represent markedly contrasting effects in both types of genetic modifications. These differences might be caused, in part, by different storage reserves available in the mobilizing respective seeds, especially in case of *TMT1* overexpressor seeds (Fig. 8, A–C).

However, accelerated development of the *TMT1* overexpressor lines might also result from improved daily net carbon usage in these mutants. Reduced carbon loss is indicated by decreased rates of Glc respiration in the three *TMT1* overexpressor lines (Fig. 6A) and decreased nocturnal respiration in the two *TMT1* overexpressor lines 4 and 10 (Fig. 9B), having the largest seeds (Fig. 8A). It is worth noting that potato (*Solanum tuberosum*) tuber cells with elevated cytosolic levels of hexoses exhibit stimulated respiratory carbon loss (Trethewey et al., 1999). Thus, physiological changes displayed by *TMT1* overexpressor lines 4 and 10 (i.e. less respiration of Glc; Fig. 6A) and reduced nocturnal CO₂ release (Fig. 9B) generally provide more cellular carbon for anabolic reactions, thereby elevating seed production.

Phloem exudates were examined to determine why *TMT1* overexpressor lines exhibit increased 1,000 seed weight and increased total seed biomass per plant (Fig. 8, A and D). Exudate analysis confirmed that the three *TMT1* overexpressor lines exhibit increased capacity to export sugars from source to sink tissue, whereas, as expected, the *tmt1-2::tDNA* double knockout plants exhibit slightly reduced phloem export rates (Fig.

10C), correlated with reduced seed yields (Fig. 8, A and B). Accordingly, we assume that after the onset of seed development in *TMT1* overexpressors, the novel sink gains more carbon than corresponding tissue in wild-type plants. Interestingly, it has recently been shown that stimulated sugar loading in developing wheat (*Triticum aestivum*) grains leads to increased seed biomass (Weichert et al., 2010). The latter observation is an example of a yield gain caused by increasing sink strength (Weichert et al., 2010), whereas the *TMT1* overexpressor lines demonstrate that elevated source strength can also stimulate seed production. It has not escaped our attention that stimulated seed weight is not only caused by altered lipid contents but also by increased seed protein levels (Fig. 8, A–C). At this point, we cannot fully explain this observation, but it seems conceivable that stimulated leaf sugar export in *TMT1* overexpressors (Fig. 10C) might also hold true for other photosynthates, like de novo synthesized amino acids. In this respect, it is worth mentioning that increased Suc uptake in developing wheat grains also stimulates total storage protein synthesis (Weichert et al., 2010).

Stimulated sugar export capacity of the three *TMT1* overexpressor lines (Fig. 10C) is associated with increased expression of the phloem-localized Suc transporter *SUC2* (Fig. 10B). Phloem-specific expression and onset of *SUC2* expression during induction of the source capacity of Arabidopsis leaves (Truernit and Sauer, 1995; Imlau et al., 1999) led to speculation that this carrier is critical for phloem loading in Arabidopsis (Williams et al., 2000). The observation that *SUC2* expression is inhibited upon Glc application (Fig. 10A) concurs with data on whole genome arrays (Zimmermann et al., 2004). It is reasonable to assume that cytosolic Glc concentrations in *SUC2*-expressing phloem cells are altered similarly in mesophyll cells (Figs. 4B and 6B). If so, changes in intracellular monosaccharide compartmentation might contribute to stimulated phloem loading in *TMT1* overexpressor leaves, which has been confirmed experimentally (Fig. 10C).

In this study, we tried to provide a quite comprehensive analysis of *TMT1*-overexpressing Arabidopsis plants. Accordingly, metabolic and physiological changes in different tissues and on plants grown under various growth conditions have been analyzed. Such a wide experimental approach was mandatory as altered sugar-sensing properties were demonstrated on liquid culture-grown Arabidopsis, allowing very controlled conditions. Alternatively, for studying of growth rates, young plants were required (Fig. 7), whereas for analysis of sugar export rates, mature leaves have been analyzed (Fig. 10). In summary of our results, we propose that the synthesis of storage products in Arabidopsis seeds might be limited by intracellular sugar allocation in source leaves. In addition, in wild-type plants, sugar signaling takes place under standard growth conditions. Increased activity of the

TMT1 protein (under the control of the cauliflower mosaic virus 35S promoter) causes increased source activity, as indicated by increased expression of photosynthesis-related genes (Fig. 6C), reduced consumption of sugars for respiration (Fig. 6A), reduced nocturnal loss of CO₂ (Fig. 9B), and increased sugar export capacity from source leaves (Fig. 10C). It will be interesting and informative to transfer this approach to crop plants in the near future. Moreover, the use of organ-specific promoters driving TMT1 expression will further allow us to clarify the processes observed in more detail.

MATERIALS AND METHODS

Growth of Arabidopsis

Wild-type and mutant Arabidopsis (*Arabidopsis thaliana*) plants were grown in a growth chamber on soil at 21°C (day and night), and light was present at 150 μmol quanta m⁻² s⁻¹ for 10 h per day (standard growth conditions). Alternatively, plants were cultivated in liquid medium according to a protocol suitable for fresh weight determination and feeding of effector molecules (Scheible et al., 2004) under short-day conditions. The seedlings were grown in liquid culture for 12 d (10 h of light, 14 h of dark), harvested, washed, and then used for fresh weight determination, metabolite quantification, and mRNA isolation. Generally, for RNA isolation and metabolite quantification, plant tissues were collected and immediately frozen in liquid nitrogen until use. Sugar extraction from Arabidopsis tissue and spectroscopic quantification were performed as described earlier (Quick et al., 1989).

Generation of TMT1 Overexpressor Mutants

We transformed a TMT1 derivative into the *tmt1-2::tDNA* mutant, in which a c-Myc tag (EQKLISEEDL) replaced the correspondingly long peptide behind amino acid 375. This c-Myc tag was introduced with the aim to quantify the recombinant TMT1 protein via immunodetection. However, the level of recombinant c-Myc-TMT1 protein in all mutants tested (lines 1, 4, and 10) was below the detection level of the commercially available c-Myc antibodies. Therefore, we decided to employ a recently established patch-clamp technique. This technique allows the demonstration of electrogenic sugar transport across Arabidopsis mesophyll vacuoles (Schneider et al., 2008).

For the generation of TMT1 overexpressor mutants containing a c-Myc tag, the TMT1-encoding sequence (inserted in pBSK) was modified by site-directed mutagenesis using the QuikChange site-directed mutagenesis kit (Stratagene). The triplet encoding Gly-376 (GGT) was substituted by the triplet GAA, Asp-377 by CAA, Asp-378 by AAA, Asp-379 by CTT, Asp-380 by ATC, Ser-381 stayed a Ser, Asp-382 by GAA, and Asn-383 by GAA by PCR. The following Asp-384 and Leu-385 stayed the same. We excised the mutated sequence by using *EcoRI* and *Clal* and inserted it into the correspondingly prepared original pHannibal vector. Then, the c-Myc-TMT1 construct was cut by *NotI* and inserted into the correspondingly prepared original pART27 vector. The correctness of all constructs was proven by complete sequencing.

Transformations of Arabidopsis were performed by the floral dip method (Clough and Bent, 1998) using *Agrobacterium tumefaciens* strain GV3101 harboring the c-Myc-TMT1 construct on the pART27 vector.

Quantification of Respiratory Use of [¹⁴C]Glc

For analyzing the [¹⁴C]Glc-driven respiratory activity, we prepared seedlings 30 min after the onset of illumination. Material from wild-type plants, the *tmt1-2::tDNA* double knockout plant, and the three TMT1 overexpressor mutants, grown for about 2 weeks in the growth chamber, were transferred into 2-mL reaction tubes filled with 0.1 mL of 100 μM [¹⁴C]Glc (at a specific activity of 0.4 μCi of 100 μL⁻¹). At the inside at the top of this tube, a small 0.5-mL reaction vessel, containing 50 μL of 1 N KOH, was fixed with grease to allow ¹⁴CO₂ absorption. The seedlings were allowed to float on the solution, and incubation was continued for 6 h in the dark. The reaction was stopped by adding 100 μL of 2 N HCl with a syringe through the closed lid. The hole in the lid was sealed with grease, and after subsequent incubation for 10 h, the

released radioactively labeled CO₂ was quantified in a scintillation counter (Hurth et al., 2005).

cDNA Clones, Northern-Blot Analysis, and qRT-PCR

For the analysis of molecular responses, we quantified the levels of mRNA encoding CAB1, NRI, or TMT1. The full-length cDNAs for CAB1 (At2g34430), NRI (At1g77760), and TMT1 (At1g20840) were amplified using a first-strand cDNA preparation as template, and the amplification products were cloned into the plasmid pBSK and sequenced.

Arabidopsis tissues for quantification of CAB1, NRI, or TMT1 mRNA were harvested and immediately transferred into liquid nitrogen. Total sample RNA was extracted using the RNeasy Plant Mini Kit (Qiagen). RNA gel-blot hybridization was carried out as given before (Thulke and Conrath, 1998). Labeling of probes was carried out using the Ready-To-Go random prime kit (Amersham-Pharmacia). After hybridization, the membranes were washed according to standard procedures, and blots were visualized by a Cyclon Phospho-Imager (Packard).

Quantitative real-time PCR was used to evaluate the expression profiles of CAB1, NRI, and SUC2. Primer sequences used to quantify CAB1 and NRI have been given elsewhere (Wormit et al., 2006); primers used to quantify SUC2 mRNA were as follows: SUC2_fwd, 5'-GGTGTGAATGGATTGGT-CGGA-3'; SUC2_rev, 5'-CCGGCACCGGAATTGGTTG-3'. A Verso cDNA kit (Thermo-Fisher Scientific) and total RNA after DNase treatment (Qiagen) were used for cDNA synthesis. The specificity of all primers designed was submitted to BLASTn search against the National Center for Biotechnology Information Arabidopsis databases, and any nonspecific primers were eliminated or redesigned. Each qRT-PCR sample contained 10 μL of Platinum SYBR Green qPCR SuperMix (Invitrogen), 1 μL of forward and reverse primers (10 mM), 2 μL of cDNA, and water to a total reaction volume of 20 μL. All samples were tested in triplicate; water was used as a control to rule out false-positive signals. Dissociation runs were performed to control for the possible formation of primer dimers. As an internal reference, the elongation factor EF-1α (At1g07930) was used. Results were obtained using the sequence detection software My1Q2.0 (Bio-Rad). The specificity of the qRT-PCR products obtained was determined on 2% agarose gels.

Patch-Clamp Analyses of Isolated Plant Vacuoles

Arabidopsis wild-type (ecotype Columbia) and mutant (35S:*tmt1;1-2* line 4 and the double mutant *tmt1-2::tDNA*) plants were grown on soil for 5 to 8 weeks in a growth chamber at 8-h/16-h day/night regime, 22°C/16°C day/night temperature, and a light intensity of 800 lux. Isolation of mesophyll protoplasts and release of vacuoles were performed as described previously (Beyhl et al., 2009). In some experiments, leaf samples without intact epidermis were incubated overnight in 100 mM Glc before protoplast preparation. In line with the convention for electrical measurements on endomembranes (Bertl et al., 1992), patch-clamp experiments were carried out in the whole-vacuole configuration essentially as described by Schulz-Lessdorf and Hedrich (1995) and Ivashikina and Hedrich (2005). Thereby, the vacuolar membrane was clamped to 0 mV. Patch pipettes prepared from Kimax-51 glass capillaries (Kimble Products) were characterized by a resistance in the range of 1.5 to 3 MΩ. Macroscopic currents were recorded at a sample acquisition rate of 2 ms with an EPC-7 patch-clamp amplifier (HEKA Electronic) and low-pass filtered at 30 Hz. Data were digitized by an ITC-16 computer interface (Instrutech), stored on a Fujitsu Siemens computer, and analyzed offline using the software programs Pulse (HEKA Elektronik) and IgorPro (Wave Metrics). Current amplitudes of individual vacuoles were normalized to the whole-vacuole membrane capacitance C_m to allow comparison of macroscopic current magnitudes among different vacuoles. Both bath and pipette media contained 200 mM KCl, 1 mM CaCl₂, and 2 mM MgCl₂. pH values were either adjusted with 10 mM HEPES-Tris to pH 7.5 or with 10 mM MES-Tris to pH 5.5. Glc treatment (50 mM) of the vacuole was achieved upon manually applying high pressure on a glass pipette filled with the Glc-containing bath solution and located in front of the respective vacuole. Glc application was held until under high-time resolution the corresponding current responses reached at least the quasi-steady-state level.

Nonaqueous Fractionation and Sugar Quantification

Subcellular fractionation was based on a procedure of Stitt et al. (1989) that was adapted for small amounts of tissue. Briefly, 100 mg of freeze-dried leaf

homogenate were suspended in 10 mL of heptane-tetrachlorethylene ($\rho = 1.3 \text{ g cm}^{-3}$) cooled on ice and repeatedly sonified for 5 s with pauses of 15 s over a time course of 12 min (Branson Sonifier 250, output control 4; Branson). The sonified suspension was passed through nylon gauze with 30- μm pore size (Eckert) and centrifuged. The sediment was resuspended in heptane-tetrachlorethylene ($\rho = 1.3 \text{ g cm}^{-3}$) and loaded on a linear gradient of heptane-tetrachlorethylene ($\rho = 1.3 \text{ g cm}^{-3}$) to tetrachlorethylene ($\rho = 1.6 \text{ g cm}^{-3}$). Initial density was increased to 1.35 g cm^{-3} for liquid cultures with the addition of Glc. After ultracentrifugation at 30,000 rpm for 3 h, the gradient was fractionated into nine 1-mL fractions that were divided into three subfractions of 0.3 mL. These were dried under vacuum, and one was used for marker enzyme determination and another for sugar analysis using HPLC. Alkaline pyrophosphatase as a marker for the plastidial compartment was measured as described by Jelitto et al. (2010), and UGPase as a cytosolic marker was measured as described by Zrenner et al. (1993). Acid phosphatase served as a marker for the vacuolar compartment (Boller and Kende, 1979).

Sugar quantification in fractionated samples was conducted by ion chromatography on a HPLC CarboPac PA1 column (Dionex) followed by amperometric quantitation as described (Zuther et al., 2004).

Gas-Exchange Measurements

Exchange rates for CO_2 were measured over complete diurnal cycles (10-h day/14-h night at a flow of 40 L h^{-1} using an infrared gas analysis system [Uras 3G; Hartmann & Braun]). Whole-rossette cuvettes made of plexiglass cylinders were sealed to the surface of rectangular plexiglass plates separating aerial from nongreen plant organs. Raw data for CO_2 concentration were converted to exchange rates per cm^{-2} leaf area by fitting a spline through measuring points taken every minute and integrating the difference between cuvette and ambient CO_2 concentrations using the MATLAB software package (version 7.6.0.324, R2008a).

Seed Analysis

Seed lipid and protein levels were quantified similar to previously optimized protocols (Reiser et al., 2004). For lipid quantification, 0.1 g of completely mature and air-dried seeds was homogenized in a mortar in liquid nitrogen. Subsequently, 1.5 mL of isopropanol was added and further homogenized. The suspension was transferred into a 1.5-mL reaction tube and incubated for 12 h at 4°C on a laboratory shaker at 100 rpm. Subsequently, samples were centrifuged at $13,000g$ for 10 min, and the supernatant was transferred into a preweighed 1.5-mL reaction tube. Tubes were incubated at 60°C for 8 h to completely evaporate the isopropanol. Subsequently, total lipid was quantified gravimetrically.

For seed protein quantification, 0.1 g of seeds was homogenized in a mortar at room temperature. Subsequently, 1,000 μL of buffer medium 1 (50 mM HEPES, 5 mM MgCl_2 , pH 7.5, 1% Triton X-100, 15% glycerol, 2% SDS, 1 mM EDTA, and 100 μM phenylmethylsulfonyl fluoride) was added and further homogenized. The suspension was transferred into 1.5-mL reaction tubes, and samples were centrifuged at $13,000g$ at room temperature for 10 min. The supernatant was transferred into new 1.5-mL reaction tubes, and proteins were quantified with bicinchoninic acid reagent (Pierce) according to the manufacturer's instructions.

For determination of entire seed weight per plant, *Arabidopsis* was grown under standard conditions. Using the seed-harvesting system Arasystem (Betatech), it was possible to obtain all seeds and to subsequently quantify their weight gravimetrically.

Phloem Exudate Analysis

To quantify sugar export from source leaves, we cut leaves from 6-week-old plants at the end of the light phase, recut the petiole ends under water, and transferred petiole ends directly into reaction vessels filled with 100 μL of 15 mM EDTA solution (pH 7.25; Tedone et al., 2004). Sugar export was allowed for 16 h in a water-saturated atmosphere. Subsequently, leaves were removed and the solutes in the reaction vessels were transferred for 3 min into a heating block (95°C) to stop enzymic conversion of export products. Sugars were quantified by HPLC. Since Suc exported is partly hydrolyzed via invertase, we quantified in addition the monosaccharides Glc and Fru. This allowed us to determine total sugar export capacity. As controls, water in the reaction vessel contained 100 μL of 5 mM CaCl_2 , leading to a complete block of export caused by callose formation (Tedone et al., 2004).

GenBank/EMBL accession numbers and Arabidopsis Genome Initiative locus identifiers for the genes mentioned in this article are as follows: *TMT1*, Z50752 and At1g20840; *TMT2*, AJ532570 and At4g35300; and *TMT3*, AJ532571 and At3g51490.

Received June 29, 2010; accepted August 10, 2010; published August 13, 2010.

LITERATURE CITED

- Aluri S, Büttner M (2007) Identification and functional expression of the *Arabidopsis thaliana* vacuolar glucose transporter 1 and its role in seed germination and flowering. *Proc Natl Acad Sci USA* **104**: 2537–2542
- ap Rees T (1994) Plant physiology: virtue on both sides. *Curr Biol* **4**: 557–559
- Bertl A, Blumwald E, Coronado R, Eisenberg R, Findlay G, Gradmann D, Hille B, Köhler K, Kolb HA, MacRobbie E, et al (1992) Electrical measurements on endomembranes. *Science* **258**: 873–874
- Beyhl D, Hörtensteiner S, Martinoia E, Farmer EE, Fromm J, Marten I, Hedrich R (2009) The *fou2* mutation in the major vacuolar cation channel TPC1 confers tolerance to inhibitory luminal calcium. *Plant J* **58**: 715–723
- Boller T, Kende H (1979) Hydrolytic enzymes in the central vacuole of plant cells. *Plant Physiol* **63**: 1123–1132
- Büttner M, Sauer N (2000) Monosaccharide transporters in plants: structure, function and physiology. *Biochim Biophys Acta* **1465**: 263–274
- Carpaneto A, Geiger D, Bamberg E, Sauer N, Fromm J, Hedrich R (2005) Phloem-localized, proton-coupled Suc carrier ZmSUT1 mediates Suc efflux under the control of the Suc gradient and the proton motive force. *J Biol Chem* **280**: 21437–21443
- Clough SJ, Bent AF (1998) Floral dip: a simplified method for *Agrobacterium*-mediated transformation of *Arabidopsis thaliana*. *Plant J* **16**: 735–743
- Daie J, Wilusz JE (1987) Facilitated transport of Glc in isolated phloem segments of celery. *Plant Physiol* **84**: 711–715
- Dancer JE, Neuhaus HE, Stitt M (1990) Subcellular compartmentation of uridine nucleotides and nucleoside-5'-diphosphate kinase in leaves. *Plant Physiol* **92**: 637–641
- Dietz KJ, Jager R, Kaiser G, Martinoia E (1990) Amino acid transport across the tonoplast of vacuoles isolated from barley mesophyll protoplasts: uptake of alanine, leucine, and glutamine. *Plant Physiol* **92**: 123–129
- Emmerlich V, Linka N, Reinhold T, Hurth MA, Traub M, Martinoia E, Neuhaus HE (2003) The plant homolog to the human sodium/dicarboxylic cotransporter is the vacuolar malate carrier. *Proc Natl Acad Sci USA* **100**: 11122–11126
- Endler A, Meyer S, Schelbert S, Schneider T, Weschke W, Peters SW, Keller F, Baginsky S, Martinoia E, Schmidt UG (2006) Identification of a vacuolar sucrose transporter in barley and Arabidopsis mesophyll cells by a tonoplast proteomic approach. *Plant Physiol* **141**: 196–207
- Farre EM, Geigenberger P, Willmitzer L, Trethewey RN (2000) A possible role for pyrophosphate in the coordination of cytosolic and plastidial carbon metabolism within the potato tuber. *Plant Physiol* **123**: 681–688
- Fettke J, Eckermann N, Tiessen A, Geigenberger P, Steup M (2005) Identification, subcellular localization and biochemical characterization of water-soluble heteroglycans (SHG) in leaves of *Arabidopsis thaliana* L.: distinct SHG reside in the cytosol and in the apoplast. *Plant J* **43**: 568–585
- Gerhardt R, Heldt HW (1984) Measurement of subcellular metabolite levels in leaves by fractionation of freeze-stopped material in nonaqueous media. *Plant Physiol* **75**: 542–547
- Heldt HW (2005) *Plant Biochemistry*. Elsevier Academic Press, Burlington, MA
- Hurth MA, Suh SJ, Kretschmar T, Geis T, Bregante M, Gambale F, Martinoia E, Neuhaus HE (2005) Impaired pH homeostasis in Arabidopsis, lacking the vacuolar dicarboxylate transporter and analysis of carboxylic acid transport across the tonoplast. *Plant Physiol* **137**: 901–910
- Imlau A, Truernit E, Sauer N (1999) Cell-to-cell and long-distance trafficking of the green fluorescent protein in the phloem and symplastic unloading of the protein into sink tissues. *Plant Cell* **11**: 309–322
- Ivashikina N, Hedrich R (2005) K^+ currents through SV-type vacuolar channels are sensitive to elevated luminal sodium levels. *Plant J* **41**: 606–614
- Jelitto T, Sonnewald U, Willmitzer L, Hajirezaei M, Stitt M (2010)

- Inorganic pyrophosphate content and metabolites in potato and tobacco plants expressing *Escherichia coli* pyrophosphatase in their cytosol. *Planta* **188**: 238–244
- Koch KE** (1996) Carbohydrate-modulated gene expression in plants. *Annu Rev Plant Physiol Plant Mol Biol* **47**: 509–540
- Lalonde S, Wipf D, Frommer WB** (2004) Transport mechanisms for organic forms of carbon and nitrogen between source and sink. *Annu Rev Plant Biol* **55**: 341–372
- Li Y, Beisson F, Pollard M, Ohlrogge J** (2006) Oil content of Arabidopsis seeds: the influence of seed anatomy, light and plant-to-plant variation. *Phytochemistry* **67**: 904–915
- Martinoia E, Kaiser G, Schramm MJ, Heber U** (1987) Sugar transport across the plasmalemma and the tonoplast of barley mesophyll protoplasts: evidence for different transport systems. *J Plant Physiol* **131**: 467–478
- Martinoia E, Maeshima M, Neuhaus HE** (2007) Vacuolar transporters and their essential role in plant metabolism. *J Exp Bot* **58**: 83–102
- Martinoia E, Rentsch D** (1992) Uptake of malate and citrate into plant vacuoles. In DT Cooke, DT Clarkson, eds, *Transport and Receptor Proteins of Plant Membranes*. Plenum Press, New York, pp 101–109
- Moore B, Zhou L, Rolland F, Hall Q, Cheng WH, Liu YX, Hwang I, Jones T, Sheen J** (2003) Role of the Arabidopsis Glc sensor HXK1 in nutrient, light, and hormonal signaling. *Science* **300**: 261–263
- Neuhaus HE** (2007) Transport of primary metabolites across the plant vacuolar membrane. *FEBS Lett* **581**: 2223–2226
- Niittylä T, Messerli G, Trevisan M, Chen J, Smith AM, Zeeman SC** (2004) A previously unknown maltose transporter essential for starch degradation in leaves. *Science* **303**: 87–89
- Pollock CJ** (1986) Fructans and the metabolism of Suc in vascular plants. *New Phytol* **104**: 1–24
- Quick WP, Siegl G, Neuhaus HE, Feil R, Stitt M** (1989) Short-term water stress leads to a stimulation of Suc synthesis by activating Suc-phosphate synthase. *Planta* **177**: 535–546
- Reiser J, Linka N, Lemke L, Jeblick W, Neuhaus HE** (2004) Molecular physiological analysis of the two plastidic ATP/ADP transporters from *Arabidopsis thaliana*. *Plant Physiol* **136**: 3524–3536
- Rentsch D, Martinoia E** (1991) Citrate transport into barley mesophyll vacuoles: comparison with malate uptake activity. *Planta* **184**: 532–537
- Rolland F, Moore B, Sheen J** (2002) Sugar sensing and signaling in plants. *Plant Cell* **14**: 185–205
- Ruiz-Medrano R, Xoconostle-Cazares B, Lucas J** (2001) The phloem as a conduit for inter-organ communication. *Curr Opin Plant Biol* **4**: 202–209
- Sauer N** (1992) Proton-sugar co-transporter in plants. In DT Cooke, DT Clarkson, eds, *Transport and Receptor Proteins of Plant Membranes*. Plenum Press, New York, pp 67–75
- Scheible WR, Morcuende R, Czechowski T, Fritz C, Osuna D, Palacios-Rojas N, Schindelasch D, Thimm O, Udvardi MK, Stitt M** (2004) Genome-wide reprogramming of primary and secondary metabolism, protein synthesis, cellular growth processes, and the regulatory infrastructure of Arabidopsis in response to nitrogen. *Plant Physiol* **136**: 2483–2499
- Schneider S, Beyhl D, Hedrich R, Sauer N** (2008) Functional and physiological characterization of Arabidopsis INOSITOL TRANSPORTER1, a novel tonoplast-localized transporter for myo-inositol. *Plant Cell* **20**: 1073–1087
- Schulz-Lessdorf B, Hedrich R** (1995) Protons and calcium modulate SV-type channels in the vacuolar-lysosomal compartment—channel interaction with calmodulin inhibitors. *Planta* **197**: 655–671
- Shiratake K, Kanamya J, Maeshima M, Yamaki S** (1997) Changes in H⁺-pumps and a tonoplast intrinsic protein of vacuolar membranes during the development of pear fruit. *Plant Cell Physiol* **38**: 1039–1045
- Smeekens S** (1998) Sugar regulation of gene expression in plants. *Curr Opin Plant Biol* **1**: 230–234
- Stitt M, Lilley R, Gerhardt R, Heldt HW** (1989) Metabolite levels in specific cells and subcellular compartments of plant leaves. *Methods Enzymol* **174**: 518–552
- Tedone L, Hancock RD, Alberino S, Haupt S, Viola R** (2004) Long-distance transport of L-ascorbic acid in potato. *BMC Plant Biol* **4**: 16
- Thom M, Komor E** (1984) Role of the ATPase of sugar-cane vacuoles in energization of the tonoplast. *Eur J Biochem* **138**: 93–99
- Thulke OU, Conrath U** (1998) Salicylic acid has a dual role in the activation of defense related genes in parsley. *Plant J* **14**: 35–42
- Trethewey RN, Geigenberger P, Hennig A, Fleischer-Notter H, Müller-Röber B, Willmitzer L** (1999) Induction of the activity of glycolytic enzymes correlates with enhanced hydrolysis of Suc in the cytosol of transgenic potato tubers. *Plant Cell Environ* **22**: 71–99
- Truernit E, Sauer N** (1995) The promoter of the Arabidopsis thaliana SUC2 Suc-H⁺ symporter gene directs expression of beta-glucuronidase to the phloem: evidence for phloem loading and unloading by SUC2. *Planta* **196**: 564–570
- Wanner LA, Junttila O** (1999) Cold-induced freezing tolerance in Arabidopsis. *Plant Physiol* **120**: 391–400
- Weber A, Servaites JC, Geiger DE, Koffler H, Hille D, Groner F, Hebbeker U, Flügge UI** (2000) Identification, purification, and molecular cloning of a putative plastidic Glc translocator. *Plant Cell* **12**: 787–802
- Weichert N, Saalbach I, Weichert H, Kohl S, Erban A, Kopka J, Hause B, Varshney A, Sreenivasulu N, Strickert M, et al** (2010) Increasing Suc uptake capacity of wheat grains stimulates storage protein synthesis. *Plant Physiol* **152**: 698–710
- Williams LE, Lemoine R, Sauer N** (2000) Sugar transporter in higher plants: a diversity of roles and complex regulation. *Trends Plant Sci* **5**: 283–289
- Wormit A, Trentmann O, Feifer I, Lohr C, Tjaden J, Meyer S, Schmidt U, Martinoia E, Neuhaus HE** (2006) Molecular identification and physiological characterization of a novel monosaccharide transporter from *Arabidopsis* involved in vacuolar sugar transport. *Plant Cell* **18**: 3476–3490
- Xiao W, Sheen J, Jang JC** (2000) The role of hexokinase in plant sugar signal transduction and growth and development. *Plant Mol Biol* **44**: 451–461
- Zimmermann P, Hirsch-Hoffmann M, Hennig L, Gruissem W** (2004) GENEVESTIGATOR: Arabidopsis microarray database and analysis toolbox. *Plant Physiol* **136**: 2621–2632
- Zrenner R, Willmitzer L, Sonnwald U** (1993) Analysis of the expression of potato uridinediphosphate-Glc pyrophosphorylase and its inhibition by antisense RNA. *Planta* **190**: 247–252
- Zuther E, Buchel K, Hundertmark M, Stitt M, Hincha DK, Heyer AG** (2004) The role of raffinose in the cold acclimation response of *Arabidopsis thaliana*. *FEBS Lett* **576**: 169–173